

RESEARCH ARTICLE

10.1029/2017JF004589

AEOLIAN MATERIAL TRANSPORT AND ITS ROLE IN LANDSCAPE CONNECTIVITY IN THE MCMURDO DRY VALLEYS, ANTARCTICA

Key Points:

- Polar and alpine deserts have diminished landscape connectivity due to limited and/or seasonal hydrological processes
- Connectivity of landscapes in the McMurdo Dry Valleys is more complex due to aeolian transport up to 100 cm above the surface
- Geochemistry of soluble salts and nutrients in aeolian material generally reflects complicated geologic and climate history of Ross Sea region

Melisa A. Diaz^{1,2} , Byron J. Adams³ , Kathleen A. Welch^{2,4} , Susan A. Welch^{1,2}, Stephen O. Opiyo⁵, Alia L. Khan^{4,6,7} , Diane M. McKnight^{4,6} , S. Craig Cary⁸, and W. Berry Lyons^{1,2} 

¹School of Earth Sciences, The Ohio State University, Columbus, OH, USA, ²Byrd Polar and Climate Research Center, The Ohio State University, Columbus, OH, USA, ³Department of Biology, Evolutionary Ecology Laboratories, and Monte L. Bean Museum, Brigham Young University, Provo, UT, USA, ⁴Institute of Arctic and Alpine Research, University of Colorado Boulder, Boulder, CO, USA, ⁵Molecular and Cellular Imaging Center-Columbus, The Ohio State University, Columbus, OH, USA, ⁶Department of Civil and Environmental Engineering, University of Colorado Boulder, Boulder, CO, USA, ⁷National Snow and Ice Data Center, University of Colorado Boulder, Boulder, CO, USA, ⁸Biological Sciences, University of Waikato, Hamilton, New Zealand

Supporting Information:

- Supporting Information S1
- Table S1
- Table S2
- Table S3

Correspondence to:

M. A. Diaz, diaz.237@osu.edu

Citation:

Diaz, M. A., Adams, B. J., Welch, K. A., Welch, S. A., Opiyo, S. O., Khan, A. L., et al. (2018). Aeolian material transport and its role in landscape connectivity in the McMurdo Dry Valleys, Antarctica. *Journal of Geophysical Research: Earth Surface*, 123, 3323–3337. <https://doi.org/10.1029/2017JF004589>

Received 12 DEC 2017

Accepted 22 NOV 2018

Accepted article online 30 NOV 2018

Published online 26 DEC 2018

Abstract

Arid regions, particularly polar and alpine desert environments, have diminished landscape connectivity compared to temperate regions due to limited and/or seasonal hydrological processes. For these environments, aeolian processes play a particularly important role in landscape evolution and biotic community vitality through nutrient and solute additions. The McMurdo Dry Valleys (MDV) are the largest ice-free area in Antarctica and are potentially a major source of aeolian material for the continent. From this region, samples were collected at five heights (~5, 10, 20, 50, and 100 cm) above the surface seasonally for 2013 through 2015 from Altna Valley, Victoria Valley, Miers Valley, and Taylor Valley (Taylor Glacier, East Lake Bonney, F6 (Lake Fryxell), and Explorer’s Cove). Despite significant geological separation and varying glacial histories, low-elevation and coastal sites had similar major ion chemistries, as did high-elevation and inland locations. This locational clustering of compositions was also evident in scanning electron microscopy images and principal component analyses, particularly for samples collected at ~100 cm above the surface. Compared to published soil literature, aeolian material in Taylor Valley demonstrates a primarily down-valley transport of material toward the coast. Soluble N:P ratios in the aeolian material reflect relative nutrient enrichments seen in MDV soils and lakes, where younger, coastal soils are relatively N depleted, while older, up-valley soils are relatively P depleted. The aeolian transport of materials, including water-soluble nutrients, is an important vector of connectivity within the MDV and provides a mechanism to help “homogenize” the geochemistry of both soil and aquatic ecosystems.

1. Introduction

Aeolian processes play an important role in the global transport of both geological and biological materials that in turn can greatly impact the biogeochemistry of ecosystems. In recent years, research has identified global winds as a pertinent force in material transport and in connecting distant environments and has detailed how this enhanced connectivity modifies depositional regions (Jickells et al., 2005; Okin et al., 2006; Vitousek et al., 1997). Precipitation on temperate landscapes maintains high hydrological connectivity, where overland flow moves soil materials into rivers and lakes on basin-wide, and even continental, scales. But arid regions, particularly those in polar and alpine environments with frozen soils, have significantly diminished landscape connectivity due to limited and/or seasonal hydrological processes (Gooseff et al., 2002). For polar desert environments, wind transport of materials may be particularly integral to landscape evolution and ecosystem vitality (Šabacká et al., 2012). Other than ephemeral streams, which may transmit liquid water 4–12 weeks annually connecting glaciers to primarily closed basin lakes, winds are a major transporter of materials (Fountain et al., 1999).

The McMurdo Dry Valleys (MDV) are the largest ice-free region in Antarctica (~4,800 km²), located in Southern Victoria Land, East Antarctica, and are geographically isolated from other dust-producing regions. This region is a network of soils, perennial ice-covered lakes, ephemeral streams, and alpine glaciers (Fountain et al., 1999). The MDV are classified as a polar desert with a mean annual temperature of –20 °C and annual precipitation of less than 5 cm water equivalent (Doran et al., 2002; Fountain et al., 2010). The ecosystems

associated with the MDV are relatively simplistic; are composed of microbial and algal communities, moss, and soil invertebrates; and are greatly affected by summer pulses of meltwater and aeolian deposition (Barrett et al., 2007; Fountain et al., 1999, 2014). Similarly, chemical weathering is limited to portions of the landscape where liquid water exists, such as stream channels, hyporheic zones, cryoconite holes, and lakes (Gooseff et al., 2002), but physical weathering aids in soil formation and is driven by winds.

Strong winds and katabatic events are an important feature of the MDV and can lead to surface modification. The winds of the MDV region are of three major types: down-valley, coastal, and drainage winds (Doran et al., 2002; Nylén et al., 2004). The latter flow down valley sides and alpine glaciers from higher elevations. Direction is generally dependent on valley orientation, except for strong katabatic events flowing from the east (Clow et al., 1988; Nylén et al., 2004). In the MDV, katabatic winds, specifically föhn winds, originate from the polar plateau (180–315°) where cold dense air sinks and flows downslope. The climate of the MDV is greatly influenced by the magnitude and frequency of föhn events (Obryk et al., 2017), with spatial variations dependent on proximity to the ice sheet (Nylén et al., 2004). These föhn events also help explain discrepancies in the expected temperature-elevation relationship-driven adiabatic lapse rate in Taylor Valley (Doran et al., 2002; Nylén et al., 2004) and are integral to material transport (Gillies et al., 2013; Lancaster, 2002).

The dynamics of winds and mass transport of aeolian material in MDV have been previously investigated (Doran et al., 2002; Lancaster, 2002; Nylén et al., 2004; Šabacká et al., 2012). Measurements of flux and subsequent deposition of material vary based on location and collection height. Šabacká et al. (2012) recorded the highest sediment fluxes in Taylor Valley at a collection height of 30 cm above the surface near the center of the valley ($289 \text{ g}\cdot\text{m}^{-2}\cdot\text{year}^{-1}$ in the Lake Hoare basin), while the lowest fluxes were measured in the upper parts of the valley ($8.5 \text{ g}\cdot\text{m}^{-2}\cdot\text{year}^{-1}$ in the Lake Bonney basin). Meanwhile, aeolian material collected 100 cm above the surface had the highest aeolian flux in the Lake Bonney basin and $<1 \text{ g}\cdot\text{m}^{-2}\cdot\text{year}^{-1}$ in the Lake Hoare basin (Lancaster, 2002). The material collected at 30 cm is predominately sand sized and is likely dominated by saltation, which helps to account for these noted transport variations (Deuerling et al., 2014; Gillies et al., 2013; Lancaster et al., 2010). Physical obstacles in the landscape of Taylor Valley, such as the Nussbaum and Bonney Riegels (~700 and 200 m above sea level, respectively), likely impede aeolian transport, which also affect fluxes (Fountain et al., 1999; Šabacká et al., 2012). The depositional rate of $0.66 \text{ g}\cdot\text{m}^{-1}\cdot\text{year}^{-1}$ (Lancaster, 2002) observed in Taylor Valley is an order of magnitude lower than those in other arid regions, such as the Tibetan Plateau (Honda et al., 2004; Wei et al., 2017; Xu et al., 2012). Therefore, although aeolian transport and deposition within the MDV are important processes for linking landscape components, compared to other arid locations, there is less material to be suspended and transported.

Previous geochemical analyses of aeolian material have used sediment trap collections at 30 cm above the ground (Deuerling et al., 2014; Šabacká et al., 2012), or examined sediments deposited on glacial and ice-covered lake surfaces (Deuerling et al., 2014; Lyons et al., 2003; Witherow et al., 2006). These studies concluded that aeolian materials were derived from local sources and that transport is effective at connecting landscape features within each lake basin but not between basins or valleys. In this paper, we analyze the water-soluble component and high-resolution scanning electron microscopy (SEM) images of 53 aeolian material samples collected from Miers, Taylor, Victoria, and Alatna Valleys (Figure 1) between 5 and 100 cm above the surface. Through an understanding of how this material varies spatially and temporally, and how the various landscape units interact with each other, potential impacts of aeolian transport on landscape connectivity can be better understood.

2. Methods

2.1. Study Sites

The MDV have been investigated as a Long-Term Ecological Research site (MCM-LTER) since 1993. Over this time, a number of locations within the Dry Valleys, especially Taylor Valley, have been the focus of integrated ecological, climatological, hydrological, limnological, and biogeochemical research (Priscu, 1995). The MDV are largely ice-free due to the Transantarctic Mountains, which impede ice flow from East Antarctica into McMurdo Sound. Lakes are generally isolated within closed basins, where major water inputs are glacial melt and losses are evaporation and sublimation (Doran et al., 2002; McKnight et al.,

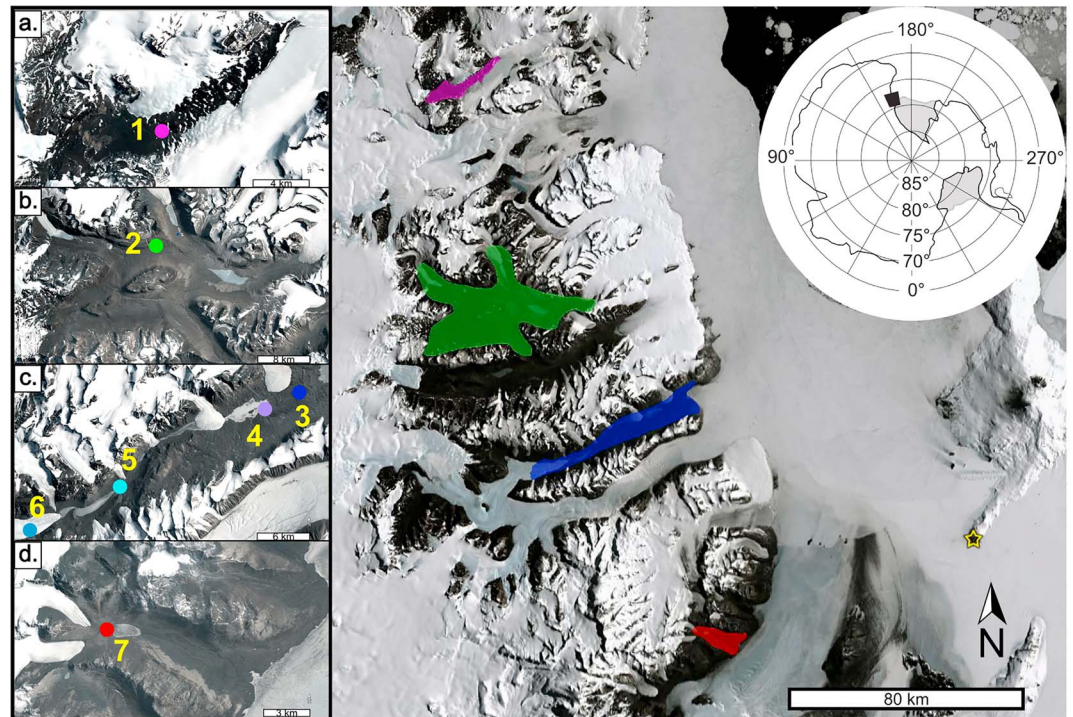


Figure 1. Landsat image of the McMurdo Dry Valleys with the four valleys of interest highlighted: Alatna Valley in magenta, Victoria Valley in green, Taylor Valley in blue, and Miers Valley in red. Specific sampling locations shown are in the four valley inset images (a)–(d). Sample locations represent a vertical transect from Alatna to Miers Valley and a horizontal transect through Taylor Valley from Explorer’s Cove to Taylor Glacier. McMurdo Station is identified as a star for reference. Further information on each site is located in Table 1.

1999). An exception is Lake Miers, the only large flow-through lake, as it drains into McMurdo Sound through Miers Stream (Figure 1d).

Located in the southern Dry Valleys, Miers Valley trends northwest to southeast at approximately 50 m above sea level. It extends from the Royal Society Range in the west to the coast of McMurdo Sound. Taylor Valley is centrally located with respect to other valleys in this study (i.e., Alatna and Miers), and it generally trends east to west. The elevations in Taylor Valley range from sea level near Explorer’s Cove at the coast to over 300 m at Taylor Glacier. Similar to Miers Valley, Taylor Valley is directly abutted to the ocean to the east. Victoria Valley is bounded to the south by the Olympus Range, to the west by the inland ice sheet, and to the north by the Clare and St. John ranges and is separated from McMurdo Sound by the Wilson Piedmont Glacier (Calkin, 1964). Victoria Valley consists of five main interlocking valleys totaling 90 km in length and generally trends northwest to southeast. It is a high-elevation valley, with the lowest elevation at approximately 350 m. Alatna Valley is located in the northernmost part of the MDV in the Convoy Range near Mackay Glacier. It is a northeast to southwest trending valley and has the highest elevation (>900 m) in this study.

The lower-elevation valleys (i.e., Miers and Taylor) have experienced dynamic change through the Pleistocene into the Holocene. During glacial maxima, the eastern ends of the valleys were “blocked” by the advance of the West Antarctic Ice Sheet, large lakes developed, and the glacial deposits were covered by the deposition of lacustrine sediments (Denton et al., 1989; Doran et al., 1994; Hall et al., 2013; Obryk et al., 2017). During interglacial periods, the East Antarctic Ice Sheet advanced seaward, while the alpine glaciers similarly advanced into the valleys (Hall et al., 1993; Wilch et al., 1993). Through the Holocene, the lake levels have fluctuated in size but have generally decreased (Hall et al., 2013; Lyons et al., 1998).

The geology of MDV is predominately composed of four main rock types. These include Cambrian/Pre-Cambrian granites and metamorphic basement; Devonian-Triassic age Beacon Supergroup strata in the Transantarctic Mountains, including a collection of sandstones, shales, conglomerates, and coal (Craddock,

Table 1
Sample Site Coordinates, Distance From the Coast and Corresponding Locations on Figure 1

Location on map	Collection site name	Latitude	Longitude	Distance from coast (km)	Elevation (m)
1	Alatna Valley	76.90008°S	161.11102°E	36	950
2	Victoria Valley	77.33092°S	161.60062°E	47	450
3	Explorer's Cove A and B	77.58873°S	163.41752°E	3.5	24
4	F6 (Lake Fryxell)	77.6085°S	163.2487°E	8.5	19
5	East Lake Bonney	77.69263°S	162.56233°E	27	64
6	Taylor Glacier	77.74002°S	162.13135°E	38.5	334
7	Miers Valley	78.09805°S	163.79423°E	10.5	50

1970; Kyle, 1990); Jurassic age Ferrar Dolerite of tholeiitic affinity (Bockheim & McLeod, 2007); and the McMurdo Volcanic Group of Cenozoic age containing basalts and quartz-free basic to felsic volcanic rocks (Kyle, 1990; Marchant & Denton, 1996). The valley floors consist of tills deposited by the movement of both the East Antarctic Ice Sheet and West Antarctic Ice Sheet, as well as local alpine glaciers (Denton et al., 1989; Hall et al., 2000). These deposits are heavily modified by aeolian, fluvial, and fluvio-glacial and limnological activity and therefore have higher amounts of sand compared to higher elevations (Prentice et al., 1998). Due to the different influences of these various physical processes over time, the till and lacustrine sediments that are now exposed vary within each valley in MDV and are potentially sources of local "dust" (Bockheim & McLeod, 2007).

2.2. Sampling and Analysis

Big Spring Number Eight isokinetic wind samplers were deployed at seven collection sites throughout the MDV. Big Spring Number Eight samplers passively collect 95% of airborne material that enters the collection box opening, regardless of wind velocity or direction (Shao et al., 1993). Though the aeolian material collection trays were initially set to standardized heights above the surface (5, 10, 20, 50, and 100 cm), strong winds generated variation in heights among the individual units. Therefore, relative elevation terms (bottom lower, bottom middle, bottom upper, middle, and top) are used in this work rather than absolute heights.

Aeolian material from Alatna, Victoria, Taylor (Explorer's Cove, F6, East Lake Bonney, and Taylor Glacier), and Miers Valleys (Figure 1) was collected seasonally in 2013 and 2014 and year-round for 2015. Fifty-three samples were obtained, with 38 samples containing more than 5 g. Samples were collected twice: once in November and again in January. November collections are termed "winter" (from 15 January to 31 October), while January collections are termed "summer" (from 1 November to 14 January). Sampler locations and coordinates are detailed in Table 1 and Figure 1.

2.2.1. Water-Soluble "Leaches"

Acid was generally avoided due to potential contamination of the samples from the dissolution of strong acids (i.e., HCl and HNO₃). For the samples with greater than 5 g of mass, 0.5 g of sample was leached with 2.5 ml of 18 Ω deionized (DI) water chilled to 3 °C, consistent with soil leaches performed by MCM-LTER researchers (e.g., Barrett et al., 2005; Nkem et al., 2006). Chilled DI water was used to represent surface water temperatures in the MDV. Recent work has clearly demonstrated that this 1:5 mass to volume ratio may not solubilize all the salts present in MDV soils (Toner et al., 2013). We strongly desired to produce data comparable to previous LTER soil measurements and hence used their soil:water ratio but modified the procedure by including a second sequential leach similar to Toner et al. (2013). Throughout sample analysis, all tubes and equipment were cleaned with several DI water rinses. Samples were agitated for 1 min by hand then set to rest at 3 °C for 30 min. This was the first of two leaches. After 30 min, the water from the first leach was extracted and filtered using a 0.45-μm Whatman® polypropylene syringe filter and stored in a clean Falcon™ tube at 3 °C in preparation for chemical analysis. The first two to three drops of leachate were discarded to minimize potential contamination from the filtration process. The second leach followed a similar procedure, but the extraction lasted for 24 hr. These two time steps were chosen to ideally simulate short pulses of water hydrating aeolian sediment in MDV to dissolve rapidly soluble solids (30 min) and long-term wetting (24 hr). Samples with ~5 g of mass were leached using the entire mass of the sample. Process blanks were produced by filtering chilled DI at ~3 °C water through a clean syringe and filter and were later analyzed along with the sample leachates. Contamination from filtering was negligible, as the measured ion and

nutrient concentrations were less than the concentrations found in the DI water (supporting information Table S1).

2.2.2. Nutrient and Ion Analysis

The water collected from the sediment leaches was separated into two aliquots. The first aliquot was analyzed for soluble reactive phosphorous (PO_4^{3-}) and nitrate plus nitrite ($\text{NO}_3^- + \text{NO}_2^-$) on a Skalar San++ Automated Wet Chemistry Analyzer with an SA 1050 Random Access Auto-sampler.

The second aliquot was used to quantify major cations (K^+ , Na^+ , Ca^{2+} , and Mg^{2+}) and anions (F^- , Cl^- , Br^- , and SO_4^{2-}). Cations were analyzed using a Dionex DX-120 ion chromatograph with an AS40 automated sampler, and anions were analyzed using a Dionex ICS-2100 ion chromatograph and an AS-DV automated sampler, as originally described by Welch et al. (1996; 2010). Alkalinity (HCO_3^-) was calculated through charge balance difference, which is the best estimate for alkalinity using this method with an average standard error of $\pm 14\%$ from MDV stream water (Lyons et al., 2012). Precision and accuracy ranged from 0.13% to 21.0% and 0.18% to 18.7%, respectively (Table S1).

2.2.3. SEM

High-resolution electron microscopy images were obtained of the uppermost collection heights ("middle" or "top") from each location with an FEI Quanta 250 Field Emission Gun scanning electron microscope (SEM) equipped with a Bruker X-Flash X-ray spectrometer and Bruker Quantax software to examine the rounding and sorting of aeolian sediment grains, grain encrustations, and any biological material present, and estimate particle size. Spot chemistry was performed using energy dispersive X-ray spectroscopy analysis with a working volume that spans $1\text{--}3 \mu\text{m}^3$ to identify specific elements and estimate mineralogy. Elemental maps on grain surfaces were also generated to detail salt encrustations, such as NaCl and CaSO_4 .

2.2.4. PCA

Principal component statistical analysis was performed using R statistical programming (R Core Team, 2013). Principal component analysis (PCA) was conducted using correlation matrix standardized data. The levels of variables representing nutrients were selected using their loading scores with cutoff ≥ 0.01 .

3. Results

3.1. Water-Soluble Geochemistry

Ion concentrations from the two sequential aeolian material leaches were summed to represent the total contributions of ions to the surface (Table 2). For anions, all sites were below the detection limit for Br^- , except for F6 (Lake Fryxell) and Explorer's Cove. Cl^- concentrations ranged between 0.161 and $19.1 \mu\text{mol/g}$. Coastal samples contained the highest concentrations of Cl^- , while more inland samples were higher in SO_4^{2-} . F6 was high in both anions. Cl^- concentrations were greatest in the uppermost collection height (top) for the inland, higher-elevation sites.

Cation concentrations did not vary as greatly as anion concentrations (Table 2). The lowest cation concentration was K^+ in Alatna Valley at $0.047 \mu\text{mol/g}$, and the highest was $23.6 \mu\text{mol/g}$ of Na^+ at F6. Na^+ is the dominant cation for all sites, followed by Ca^{2+} , then Mg^{2+} and K^+ . The down-valley locations of F6 and Explorer's Cove had the highest concentrations of Na^+ , while inland samples had relatively more Ca^{2+} . The upper collection height samples generally had higher concentrations of Na^+ and Mg^{2+} than lower collection height samples, but similar trends were not observed for K^+ and Ca^{2+} . The 2015 full-year samples at Explorer's Cove, which likely reflect a more summer influence due to strong coastal breezes, contained the highest concentrations of Na^+ , while winter samples from the inland locations were locally higher.

Nutrient concentrations varied greatly between samples, often greater than an order of magnitude (Table 2). The highest NO_3^- concentration was in the uppermost sample at Taylor Glacier ($0.411 \mu\text{mol/g}$), while the lowest NO_3^- concentration was in the lowest sample height at Explorer's Cove ($0.006 \mu\text{mol/g}$). PO_4^{3-} concentrations were at or below the detection limit for some inland and high-elevation locations ($<0.0001 \mu\text{mol/g}$) but ranged as high as $0.0105 \mu\text{mol/g}$ at the coast. Winter and uppermost samples had the highest concentrations of NO_3^- for all sites, while middle- to low-level ("bottom middle" and "bottom upper") samples had the highest concentrations of PO_4^{3-} .

Table 2

Concentrations of Water-Soluble Major Ions and Nutrients in McMurdo Dry Valleys Aeolian Material, Determined by Ion Chromatography and Nutrient Analysis in Micromoles per Gram From 1:5 Sediment to Water Leach

Site	Height	Year	F ⁻	Cl ⁻	Br ⁻	SO ₄ ²⁻	Na ⁺	K ⁺	Mg ²⁺	Ca ²⁺	NO ₃ ⁻	PO ₄ ³⁻
Alatna	Bottom lower	Winter 2013	0.043	0.310	—	1.03	2.35	0.047	0.380	0.642	0.258	0.0026
Alatna	Bottom middle	Winter 2013	0.043	0.424	—	0.395	1.37	0.106	0.203	0.338	0.276	0.0003
Alatna	Middle	Winter 2013	0.037	1.08	—	1.26	3.65	0.058	0.465	1.23	0.268	0.0004
East Lake Bonney	Bottom lower	Winter 2014	0.020	5.58	—	1.63	4.87	0.366	1.44	2.06	0.079	—
East Lake Bonney	Bottom middle	Winter 2014	0.015	3.84	—	1.09	3.55	0.283	1.05	1.52	0.061	—
East Lake Bonney	Bottom upper	Winter 2014	0.027	5.57	—	1.54	5.75	0.361	1.39	2.16	0.068	0.0012
East Lake Bonney	Middle	Winter 2014	0.025	4.41	—	1.28	4.71	0.321	1.28	1.88	0.066	0.0016
East Lake Bonney	Top	Winter 2014	0.023	3.07	—	0.570	3.49	0.248	0.838	1.27	0.043	0.0008
East Lake Bonney	Bottom lower	2015	0.016	2.38	—	0.602	2.68	0.183	0.744	1.02	0.035	0.0025
East Lake Bonney	Bottom middle	2015	0.019	2.45	—	0.512	2.88	0.205	0.819	1.10	0.036	0.0028
East Lake Bonney	Bottom upper	2015	0.015	2.60	—	0.839	3.02	0.219	0.794	1.46	0.036	0.0027
East Lake Bonney	Middle	2015	0.022	2.92	—	1.20	3.40	0.259	0.963	1.66	0.043	0.0027
East Lake Bonney	Top	2015	0.023	2.29	0.003	1.09	3.20	0.248	0.962	1.72	0.030	0.0028
Explorer's Cove B	Middle	Winter 2013	0.007	1.45	—	0.620	4.16	0.198	0.240	0.518	0.035	0.0017
Explorer's Cove A	Bottom lower	2015	0.026	6.75	0.010	0.563	10.9	0.368	0.454	0.492	0.023	0.0050
Explorer's Cove A	Bottom middle	2015	0.022	2.22	0.002	0.523	5.78	0.237	0.203	0.336	0.017	0.0069
Explorer's Cove A	Bottom upper	2015	0.037	5.53	0.005	0.560	10.3	0.343	0.298	0.422	0.031	0.0114
Explorer's Cove A	Middle	2015	0.034	2.73	0.001	0.471	6.98	0.257	0.161	0.362	0.027	0.0128
Explorer's Cove A	Top	2015	0.029	2.76	0.002	0.496	7.21	0.265	0.143	0.336	0.029	0.0147
Explorer's Cove B	Bottom lower	Winter 2014	0.024	0.735	—	0.271	4.34	0.188	0.121	0.369	0.006	0.0123
Explorer's Cove B	Bottom middle	Winter 2014	0.023	1.33	0.010	0.247	4.61	0.191	0.071	0.317	0.007	0.0150
Explorer's Cove B	Bottom upper	Winter 2014	0.026	0.627	0.002	0.262	5.73	0.179	0.055	0.285	—	—
Explorer's Cove B	Middle	Winter 2014	0.028	6.82	0.007	0.563	11.9	0.355	0.227	0.520	0.028	0.0105
Explorer's Cove B	Top	Winter 2014	0.026	8.18	0.009	0.659	12.9	0.379	0.445	0.689	0.035	0.0076
Explorer's Cove B	Bottom lower	2015	0.021	2.76	0.001	0.392	5.96	0.290	0.255	0.394	0.022	0.0063
Explorer's Cove B	Bottom middle	2015	0.033	10.8	—	0.638	15.5	0.505	0.686	0.575	0.049	0.0071
Explorer's Cove B	Bottom upper	2015	0.022	2.45	—	0.387	5.88	0.241	0.162	0.384	0.021	0.0078
Explorer's Cove B	Middle	2015	0.033	2.85	—	0.352	7.24	0.269	0.176	0.386	0.033	0.0127
Explorer's Cove B	Top	2015	0.039	3.30	—	0.360	8.18	0.289	0.196	0.376	0.037	0.0138
F6 (Lake Fryxell)	Bottom lower	Summer 2013/2014	0.024	5.07	0.015	0.838	8.40	0.413	0.526	0.956	0.107	0.0032
F6 (Lake Fryxell)	Bottom middle	Summer 2013/2014	0.017	4.37	0.016	0.773	7.34	0.388	0.511	1.08	0.093	0.0025
F6 (Lake Fryxell)	Bottom upper	Summer 2013/2014	0.016	1.84	0.016	0.568	4.72	0.262	0.219	0.583	0.037	0.0037
F6 (Lake Fryxell)	Middle	Summer 2013/2014	0.017	6.36	0.035	0.634	7.53	0.403	0.750	0.923	0.078	0.0003
F6 (Lake Fryxell)	Top	Summer 2013/2014	0.039	18.9	0.052	1.87	17.2	1.02	2.79	2.64	0.241	0.0019
F6 (Lake Fryxell)	Bottom upper	Winter 2014	0.042	15.1	0.007	1.28	18.7	0.661	0.812	0.769	0.178	0.0068
F6 (Lake Fryxell)	Middle	Winter 2014	0.058	11.6	0.006	1.42	16.8	0.632	0.495	0.521	0.147	0.0112
F6 (Lake Fryxell)	Top	Winter 2014	0.050	19.1	0.017	1.09	23.6	0.870	0.882	0.655	0.184	0.0042
Miers	Bottom lower	Summer 2013/2014	0.010	0.647	—	0.317	1.87	0.184	0.111	0.659	0.030	—
Miers	Bottom middle	Summer 2013/2014	0.013	0.367	—	0.328	1.31	0.180	0.104	0.800	0.025	0.0006
Miers	Bottom upper	Summer 2013/2014	0.011	0.323	—	0.356	1.27	0.171	0.082	0.766	0.022	0.0009
Miers	Middle	Summer 2013/2014	0.013	0.318	—	0.278	1.17	0.165	0.073	0.752	0.016	0.0007
Miers	Top	Summer 2013/2014	0.010	0.300	—	0.261	1.04	0.154	0.059	0.687	0.015	0.0002
Miers	Bottom upper	Summer 2014/2015	0.007	0.380	—	0.302	1.19	0.108	0.088	0.766	0.029	0.0009
Miers	Middle	Summer 2014/2015	0.008	0.372	—	0.361	1.46	0.129	0.118	0.763	0.033	0.0003
Taylor Glacier	Bottom lower	Winter 2014	0.007	2.04	—	0.486	2.89	0.091	0.246	0.725	0.232	0.0002
Taylor Glacier	Bottom middle	Winter 2014	0.010	1.95	—	0.458	2.91	0.090	0.240	1.02	0.217	0.0003
Taylor Glacier	Bottom upper	Winter 2014	0.007	1.83	—	0.455	2.69	0.080	0.201	0.774	0.238	0.0023
Taylor Glacier	Middle	Winter 2014	0.018	3.91	—	1.05	4.47	0.138	0.471	1.80	0.411	0.0010
Victoria	Bottom lower	Winter 2013	0.013	0.924	—	0.842	2.57	0.104	0.269	1.45	0.282	0.0000
Victoria	Bottom middle	Winter 2013	0.016	1.60	—	0.852	3.17	0.152	0.420	1.41	0.340	0.0002
Victoria	Bottom upper	Winter 2013	0.005	0.161	—	0.301	0.951	0.063	0.072	0.605	0.041	0.0014
Victoria	Middle	Winter 2013	0.007	1.03	—	0.503	2.13	0.113	0.174	1.08	0.151	0.0010
Victoria	Top	Winter 2013	0.012	2.11	—	0.904	3.96	0.130	0.172	1.21	0.280	—

Note. Values are the sum of two sequential 30-min and 24-hr leaches. Dashes represent measurements below the detection limit.

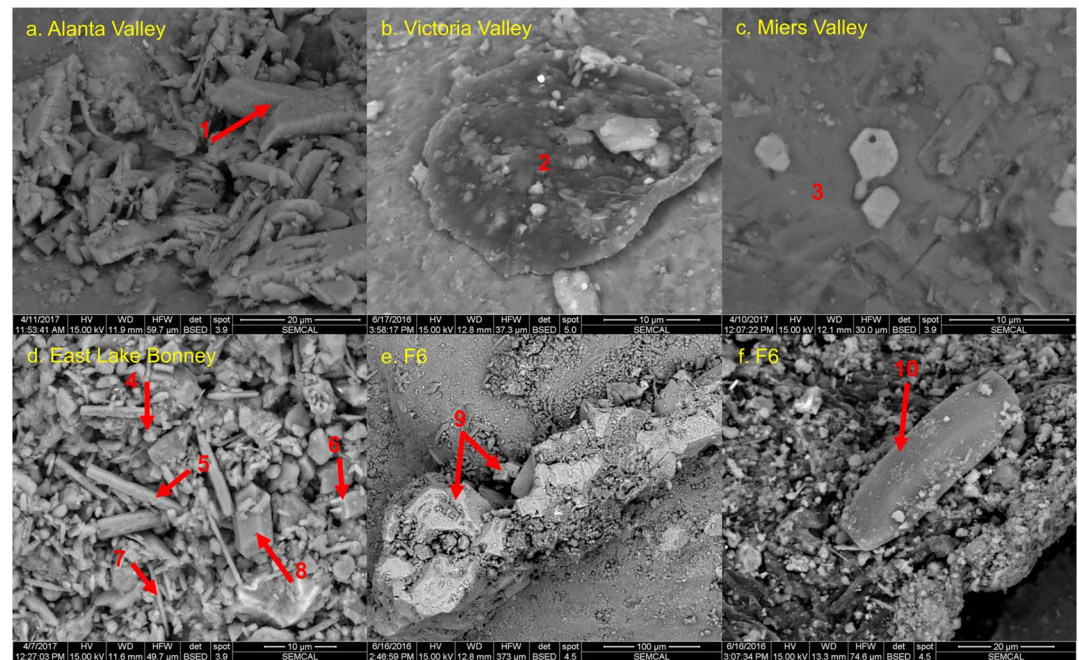


Figure 2. Scanning electron microscope imaging detailing grain encrustations and chemistry using energy dispersive X-ray spectroscopy. Red arrow and numbers indicate materials described in sections 3 and 4. 1 = gypsum ($\text{CaSO}_4 \cdot 2\text{H}_2\text{O}$); 2 = a carbon flake; 3 = volcanic glass; 4 = mirabilite ($\text{Na}_2\text{SO}_4 \cdot 10\text{H}_2\text{O}$); 5 = magnesium carbonate (MgCO_3); 6 = halite (NaCl); 7 = glauberite ($\text{Na}_2\text{Ca}(\text{SO}_4)_2$); 8 = calcium carbonate (CaCO_3); 9 = halite (NaCl); 10 = frustule of the diatom *Hantzschia amphioxys*. (a) Alanta Valley, (b) Victoria Valley, (c) Miers Valley, (d) East Lake Bonney, and (e, f) F6.

3.2. Grain Size, Composition, and Encrustations From Scanning Electron Microscopy

Energy dispersive X-ray spectroscopy was used to examine grain composition and encrustation chemistry. Samples from Alanta and Victoria Valleys were composed of rock segments ranging from <250 to $750 \mu\text{m}$ in size, which were fairly well sorted and angular. Many grains were encrusted with salts, predominately gypsum ($\text{CaSO}_4 \cdot 2\text{H}_2\text{O}$), mirabilite ($\text{Na}_2\text{SO}_4 \cdot 10\text{H}_2\text{O}$), and glauberite ($\text{Na}_2\text{Ca}(\text{SO}_4)_2$); Figure 2a), and had Fe staining. Particles composed of trace metals (Pb, Sn, Bi, and W) were observed as surface flecks, with concentrations suggesting an anthropogenic source. On some grains, carbon-rich particles were observed (Figure 2b), which could either be soot from fossil fuel combustion (Khan et al., 2016; Lyons et al., 2000), evidenced by the lack of structure, or from algal mats (Moorhead et al., 1999)

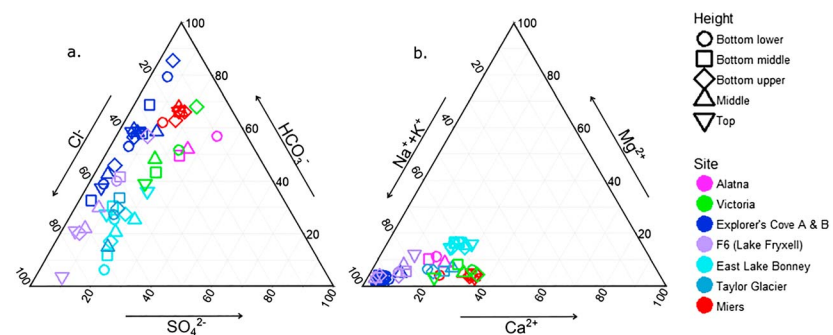


Figure 3. Anion (a) and cation (b) variation diagrams with ions as a percent of the total major constituents. HCO_3^- concentration was determined by charge balance. The colors in the key correspond to valley colors in Figure 1 and are uniform for all following figures.

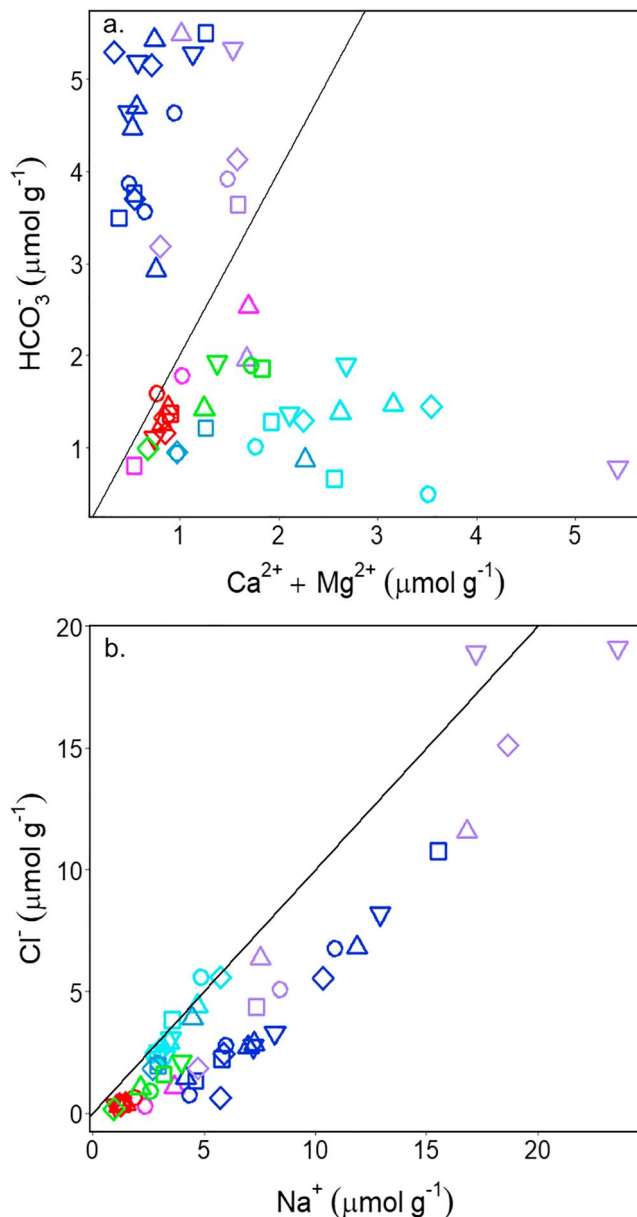


Figure 4. Spatial distribution of alkaline earth enriched McMurdo Dry Valley aeolian material (a). The black line represents the 1:2 carbonate dissolution line. Na^+ and Cl^- distribution of McMurdo Dry Valley aeolian material (b). The black line represents the 1:1 halite dissolution line.

Miers Valley had the highest occurrence of volcanic rock fragments, ash, and glass compared to all other locations (Figure 2c). The grains were a mixture of round and angular and ranged from 100 to 1,000 μm in size. Overall, the mafic chemistry of mineral grains in Miers Valley suggest a dolerite source.

The grains at East Lake Bonney and Taylor Glacier were better sorted and ranged from 250 to 750 μm . The surfaces of the grains demonstrated extensive alteration, where minerals such as feldspars were weathered to needles. Other sediment grains had deep etch pits filled with salts, such as halite (NaCl), mirabilite, glauberite, and gypsum at East Lake Bonney and predominately gypsum at Taylor Glacier (Figure 2d).

The grains at Explorer's Cove and F6 ranged from <100 to 1,000 μm and were rounded and weathered. The grains themselves were predominately encrusted with halite or gypsum (Figure 2e). Compared to the high-elevation sites of Victoria and Alatna Valleys, Explorer's Cove and F6 had more volcanic materials, including volcanic ash, many of which had been weathered on the outer edges. Within the small segments of weathered minerals, microorganism remains were present, including frustules of diatoms, such as *Hantzschia amphioxys* at Explorer's Cove (Figure 2f) and *Muelleria meridionalis* at F6.

4. Discussion

Previous studies on aeolian dust transport in the MDV have shown that wind is an important distributor of organic matter and nutrients and is a modifier of biodiversity that contributes to aquatic ecosystem vitality (Deuerling et al., 2014; Šabacká et al., 2012). Aeolian deposition of potentially soluble nutrients associated with particulate matter may be important in supporting biological communities along lake edges, where deposition to the surface of lakes is believed to be a source of organic carbon to deeper waters (Adams et al., 1998; Fristen et al., 2000). MDV winds can also add black carbon to the water column, which is resuspended from the valley floor, and may influence a shift toward an anthropogenic chemical signature of black carbon in lake surface waters (Khan et al., 2016). In ice-covered environments, such as lake ice and glacier surfaces, portions of the aeolian material can be solubilized, adding nutrients and other solutes to the aquatic ecosystem (Bagshaw et al., 2007; Deuerling et al., 2014; Lyons et al., 2003; Porazinska et al., 2004). Similarly, stream channels, which are dry most of the year, collect aeolian material and release solutes during summer melting (Barrett et al., 2007; Lyons et al., 1998).

4.1. Aeolian Composition—Water-Soluble Component

Deuerling et al. (2014) analyzed aeolian material from lake and glacier ice (11 sites), elevated sediment traps at 30 cm (three sites), and aeolian landforms (four sites). They found the highest concentrations of total dissolved solids in the aeolian material collected in sediment traps compared to the ice surfaces. They interpreted this to mean that the aeolian trap material had not been in previous contact with the hydrological system (i.e., liquid water), while the material from the ice surfaces had been in contact with water and had lost some of its original soluble component. Their sediment trap water leaches were enriched in Na^+ plus K^+ , while aeolian material collected from landforms and ice had relatively higher Ca^{2+} and Mg^{2+} concentrations (Deuerling et al., 2014). The analysis of aeolian material presented here similarly demonstrates high concentrations of water-leachable Na^+ plus K^+ , suggesting that these cations are associated with the most soluble salts and are the first to solubilize with wetting (Figure 3). During sequential leach experiments, Toner et al. (2013) found that the majority of Na^+ and K^+ from Taylor Valley soils was solubilized in the initial wetting, regardless of the water to solid ratio used to solubilize the salts, while Ca^{2+} and

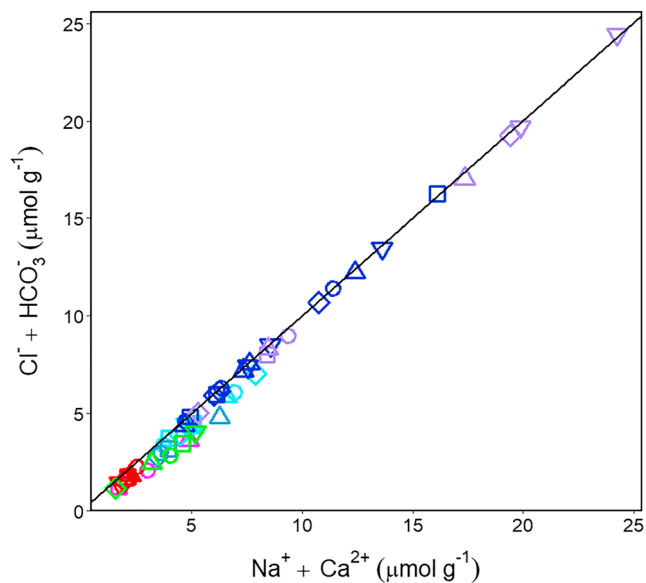


Figure 5. Major anions and cations associated with common salts on McMurdo Dry Valley aeolian material. Black line represents a 1:1 dissolution line.

Mg^{2+} increased with increasing water contact. These results suggest that Ca^{2+} and Mg^{2+} are mostly associated with less soluble SO_4^{2-} and CO_3^{2-} salts, likely in the form of mirabilite, glauberite, gypsum, calcium carbonate, and magnesium carbonate as seen in SEM images (Figure 2). The cation distribution of sediment on aeolian landforms from Deuerling et al. (2014) was similar to their sediment trap material when compared to the ice surface materials. Particles on ice surfaces have the most potential for contact with liquid water, while the low precipitation and high sublimation rates of fallen precipitation on landform surfaces probably result in only minor wetting, which may explain why the landforms and entrained material are relatively more enriched in Na^+ and K^+ compared to ice surfaces.

4.2. Spatial Variability—Locational Clustering

Though Na^+ plus K^+ were the major soluble cation constituents for all samples (Figure 3), the soluble chemistry of the samples still varies with location, specifically with distance from McMurdo Sound, and with elevation. Further, inland and high-elevation sites were most similar to each other, while low-elevation and coastal sites clustered in a ternary diagram (Figure 3). The samples from Explorer's Cove have the highest percentages of Na^+ plus K^+ at nearly 100% of the total cations, while F6 is at about 80%, East Lake Bonney at 60%, and Taylor Glacier at 70% (Figure 3). This

decreasing pattern generally follows a horizontal transect from the coast inland toward the Transantarctic Mountains. Miers, Victoria, and Alatna Valley samples were similar in their cation distribution, with minor differences in Ca^{2+} and Mg^{2+} contributions. (Figure 3).

When compared to winter samples, the summer and full-year samples in Taylor Valley were slightly more enriched in Ca^{2+} (Table 2). This may suggest that there is seasonal variability in the source of aerosols and the difference in geochemistry reflects changes from a predominately west to east wind direction. Fortner et al. (2005) observed similar effects on the surface chemistry of Canada Glacier where western proglacial streams had higher $\text{Ca}^{2+}:\text{Cl}^-$ ratios than the eastern proglacial streams. There are not enough sampling locations (i.e., up- vs. down-valley) to conclude whether such trends also exist in the other valleys.

The distributions of anions varied much more greatly than the cations, particularly in Taylor Valley. The major anions were Cl^- and HCO_3^- at all locations with SO_4^{2-} having the lowest percentage. Even at the coastal site of Explorer's Cove, Cl^- varied from between 10% to nearly 70% of the major anions (Figure 3), again suggesting different origins. F6 had a similar range. The distant and higher-elevation sites had similar anion distributions between East Lake Bonney and Taylor Glacier, as well as between Miers, Victoria, and Alatna Valleys. In these locations, HCO_3^- is the major anion, likely associated with calcium carbonate, as this mineral is found in all MDV soils (Foley et al., 2006; Toner et al., 2013). Deuerling et al. (2014) and Bisson et al. (2015) observed similar variable distribution of major anions associated with aeolian material and soils in Taylor Valley. They attributed the higher concentrations of SO_4^{2-} , particularly in the Bonney Basin, to more abundant concentrations of gypsum there. Though there was gypsum observed in grain etch pits from SEM imaging (Figure 2d), it was not the only salt present at East Lake Bonney, and the leachate from these samples suggests that Cl^- is the dominant anion, not SO_4^{2-} . Bisson et al. (2015) also observed sodium bicarbonate in Taylor Valley soils, which may contribute a minor amount of bicarbonate salts to these samples. In general, these studies agreed with the earlier work on MDV soils by Keys and Williams (1981), who first described the trends of soluble salts in Taylor Valley soils.

The wide range of anion contributions is likely due to several factors: (1) variations in wind direction and hence material source throughout the year (Nylen et al., 2004), (2) differences in the chemistry of material at different collection heights above the surface due to grain size and density or other transport-related differences (Lancaster, 2002), and (3) the "dryness" of the local/regional provenance which is usually related to the age of the surface (Lyons et al., 2016). At Explorer's Cove in eastern Taylor Valley, samples have a greater percentage of HCO_3^- in the winter compared to the full-year samples. In western Taylor Valley, the seasonal

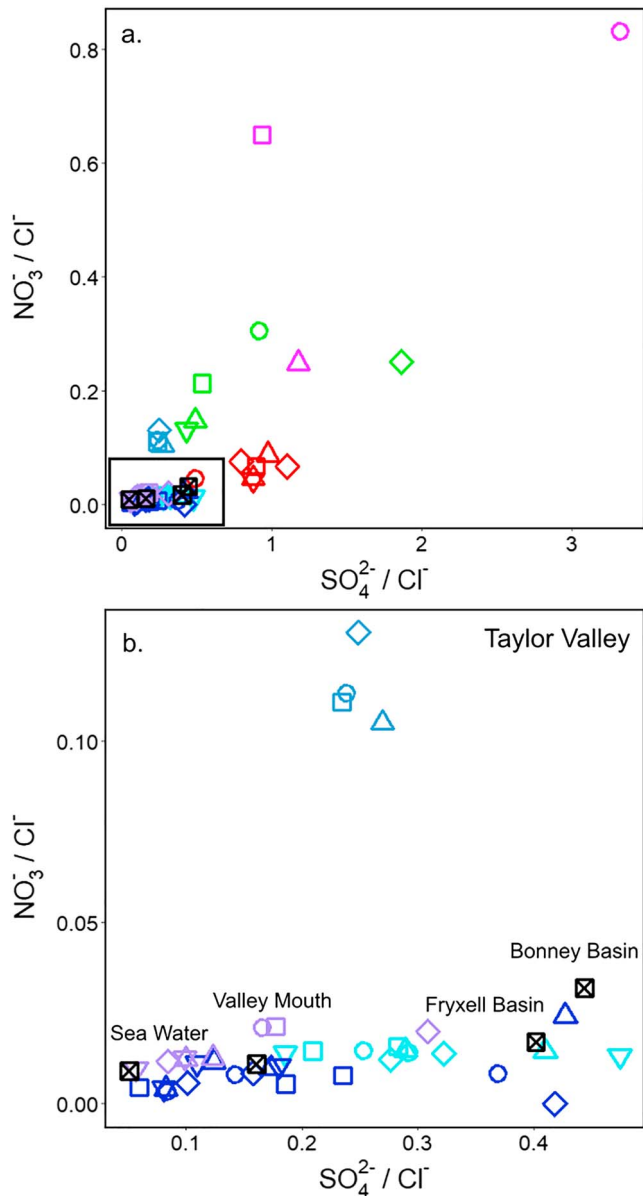


Figure 6. Molar concentrations of SO_4^{2-} and NO_3^- normalized to Cl^- for all valleys (a). Aeolian material from Taylor Valley is compared to published average soil salt distributions in Taylor Valley (Toner et al., 2013), shown as crossed boxes (b).

variability at East Lake Bonney was the opposite with winter samples having less HCO_3^- compared to full-year samples (Table 2). This is likely due to stronger up-valley winds near Explorer's Cove during summer months (Nylen et al., 2004), which have a more marine aerosol chemical signature.

Topmost samples from the aeolian collector (~100 cm above the surface) also tended to deviate from this more general anion clustering based on location. Anion content for F6 top is approximately 90% Cl^- , where all other lower collection heights are less than 80%. Top samples from East Lake Bonney and Victoria Valley are nearly identical in their anion distributions and have a similar percentage (~20%) of SO_4^{2-} as Alatna Valley top (Figure 3). Though the variations are not large, these differences are likely indicative of different types, either size or source, of aeolian material being transported in Taylor Valley that vary depending on height above the ground. Lancaster (2002) found that the grain size of aeolian sediment transported at 100 cm above the surface varied between 10% and 99% sand, with the remainder mainly silt. Deuerling (2010) found that all aeolian collections at 30 cm above the surface were dominated by sand-sized or even larger particles, and some even had as high as 60% gravel by weight. The difference in grain size with height above the ground surface in these studies indicates different material at different heights and may explain differences in soluble chemistry between top and bottom samples in this study. Because it was not possible to perform sieve-based grain size analysis of the samples due to a lack of sufficient mass and the potential risk of contamination (though a general overview of particle size is discussed in section 3), it is unclear if the differences in chemistry are just reflected in the sizes of the materials transported or are real differences in sources.

While samples from the coastal and low-elevation sites of Explorer's Cove and F6 were more enriched in HCO_3^- , the distant and higher-elevation samples were more alkaline earth enriched (Figure 4). The higher concentrations of HCO_3^- corroborate more carbonate source material. The Ca^{2+} and Mg^{2+} concentrations measured in the water leaches are likely due to the dissolution of Mg- and Ca-bearing carbonate phases (Keys & Williams, 1981), as also identified in SEM images (Figure 2). The landscape surfaces at Explorer's Cove and F6 are the youngest examined (Hall et al., 2000), and the high HCO_3^- may reflect more abundant carbonate minerals there. Keys and Williams (1981) previously observed similar trends in Taylor Valley soils, which they attributed to enhanced Mg-silicate weathering with distance from the coast. However, this trend of high Mg concentrations inland was only observed in Taylor Valley (Table 2) and not for Victoria and Alatna Valleys.

The strong association between Na^+ and Cl^- concentrations in F6 and Explorer's Cove samples suggests that these ions are from NaCl dissolution (Figures 2 and 4). The noncoastal sites have more Na^+ and Ca^{2+} compared to Cl^- and HCO_3^- , likely from sodium and calcium sulfate salts, such as gypsum, mirabilite, and glauberite (Figure 2; Bisson et al., 2015). Nearly all samples, regardless of location, have Na^+ concentrations above the NaCl dissolution line (Figure 4), suggesting a relative enrichment of Na^+ relative to Cl^- . This relationship was also observed for aeolian samples collected at 30 cm above the surface by Deuerling et al. (2014). Mirabilite is a ubiquitous salt phase within MDV soils (Bisson et al., 2015), so the additional Na^+ is thought to be in part from this source (Figure 2). Since F6 and Explorer's Cove plot directly on the combined halite and calcium carbonate dissolution line (Figure 5), it is possible that some of the Na^+ is from the dissolution of sodium bicarbonate (NaHCO_3), which Toner et al. (2013) believes could form in Eastern Taylor Valley soils (i.e., Fryxell and Hoare basins) due to the relatively higher soil moisture content. In these CaCO_3 -rich soils,

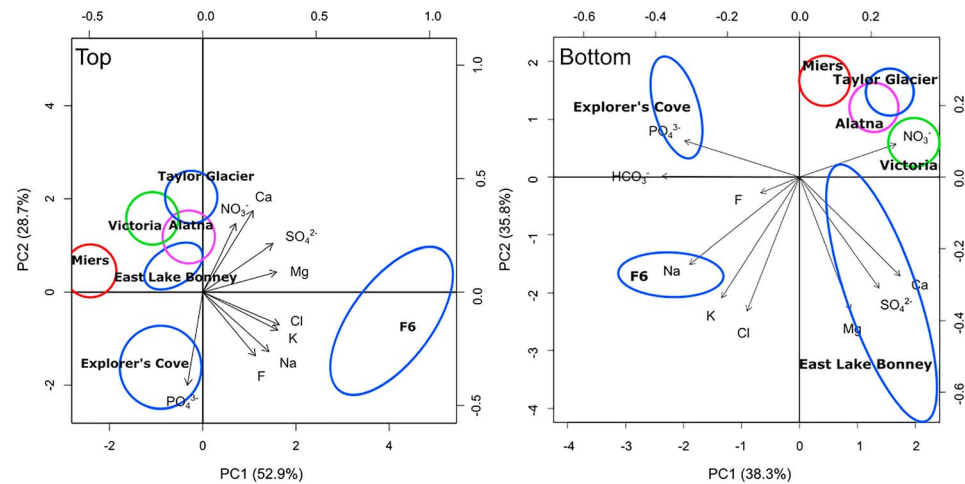


Figure 7. Principal component analysis loading plots for the top and bottom lower collection heights. Analytes are shown as eigenvectors. Colored circles represent the distribution of the sample locations. The middle collection height is plotted for Taylor Glacier and Alatna Valley for the top loading plot. Principal components 1 and 2 explain more than 50% of the variation between sample groups and represent the X and Y axes.

sodium bicarbonate forms through the dissolution of halite and calcium carbonate and then the exchange of these cations on mineral surfaces (Kelley, 1951). Once Na^+ displaces Ca^{2+} , this introduces Ca^{2+} into solution, forming CaCl_2 -rich brines, which have been observed throughout the MDV (Dickson et al., 2013; Levy et al., 2012; Lyons & Mayewski, 1993; Toner et al., 2013; Wilson, 1979).

4.3. Down-Valley Transport

The transport of material containing NaHCO_3 is likely derived primarily from the Fryxell Basin (Toner et al., 2013), perhaps suggesting down-valley material transport to the coastal site of Explorer's Cove or production of NaHCO_3 in situ there. Ratios of leachable SO_4^{2-} and NO_3^- to Cl^- also support this assertion, particularly when compared to local surface soils analyzed by Toner et al. (2013; Figure 6). Coastal samples are likely a mixture of strong down-valley wind signatures, which can overprint prominent local sources (Lancaster et al., 2010; Nylén et al., 2004), and a marine signature that remains near the coast potentially due to transport restriction from Coral Ridge, a saddle 78 m above sea level between F6 and Explorer's Cove. The composition of soils near the valley mouth is most similar to the full-year, middle-level collection height samples from Explorer's Cove, which supports the premise that locally derived resuspension of soil controls aeolian deposition there. Samples from the inland locations in Taylor Valley, particularly the winter, topmost collection height samples, suggest a more down-valley transport trend, where the aeolian sediment collections do not have the same soluble chemistry as nearby soils (Figure 6).

The highest-elevation sites (Alatna Valley, Victoria Valley, and Taylor Glacier) can be easily distinguished from the lower-elevation locations in Taylor Valley and follow an almost linear increasing trend in both SO_4^{2-} and NO_3^- from lowest to highest elevation (Figure 6). This is also similar to observations of water-soluble salts in soils from throughout the Transantarctic Mountains, where the highest-elevation soils are enriched in NO_3^- , while coastal and low-elevation soils are enriched in Cl^- (Bockheim & McLeod, 2007; Keys & Williams, 1981; Lyons et al., 2016). Isotopic analysis suggests that NO_3^- is deposited through both tropospheric and stratospheric sources, and these soluble nitrate salts accumulate on the surface because the high-elevation sites do not experience any significant liquid water (Lyons et al., 2016).

A PCA was performed for the topmost and bottommost samples from all locations and for all analytes. The locations clustered and separated based on the dominant ion chemistry, which varied based on height above the surface (Figure 7). Coastal, low-elevation locations had similar cluster patterns, while inland, high-elevation locations clustered separately. This may be due, in part, to similar glacial histories within the valleys (e.g., Alatna and Victoria Valleys are both fairly hydrologically unaltered) but does not explain all observations

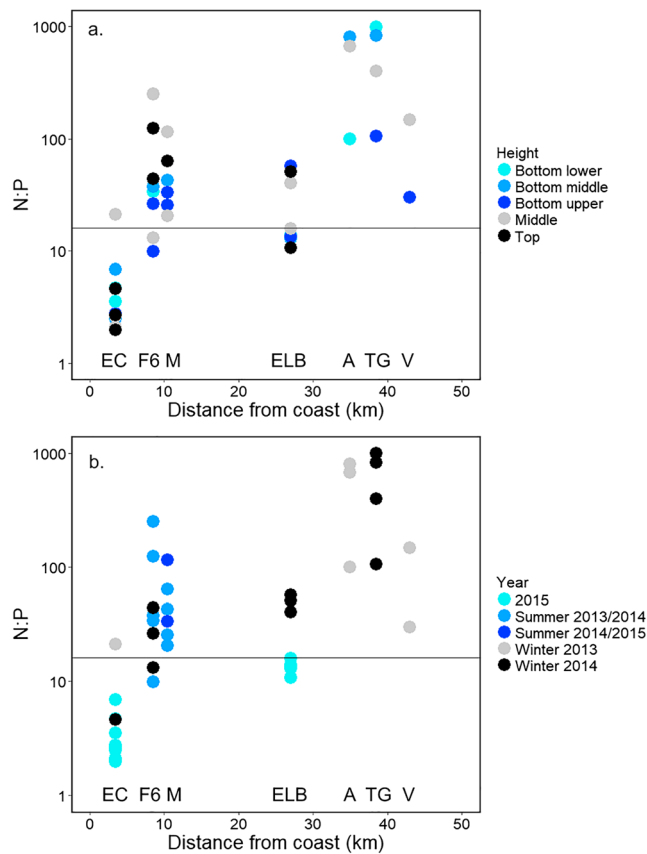


Figure 8. Molar ratios of NO_3^- to PO_4^{3-} of all McMurdo Dry Valley aeolian material. Locations are ordered by distance from the coast (km) for Explorer's Cove (EC), F6 Miers (M), East Lake Bonney (ELB), Alatna Valley (A), Taylor Glacier (TG), and Victoria Valley (V). The solid black line represents the Redfield ratio of 16:1 for N:P. Values above the line indicate P limitations relative to N, while values below the line indicate N limitations relative to P. Color gradients are used to represent collection height variations (a) and season (b).

(e.g., the difference in nutrient limitations at East Lake Bonney and the similarities between high-elevation sites in Taylor Valley and Alatna and Victoria Valleys).

4.4. Nutrient Limitations

Interestingly, the Dry Valleys exhibit similar phosphorus and nitrogen deficiencies related to landscape age as observed in the humid tropics (Chadwick et al., 1999; Vitousek et al., 1997), that is, the “younger” landscapes in Taylor Valley, such as the easternmost Ross Sea Drift tills, are more N limited while the “older” landscapes, such as the westernmost Bonney Drift tills, are more P limited (Barrett et al., 2007). In general, the water-soluble concentrations of nutrients (N and P) in the lower-elevation aeolian material are at least 2 orders of magnitude lower than soluble major ion concentrations. Thus, the input of aeolian material with different water-soluble N:P ratios could have important ramifications on the structure and function of both aquatic and soil ecosystems (Barrett et al., 2007). Topmost samples from F6 and Miers Valley were generally N enriched, while Explorer's Cove top samples were the most P enriched (Figure 8). This observation further supports a down-valley transport pattern from Taylor Glacier toward F6, as it reflects the observed differences in Bonney Basin versus Fryxell Basin soils (Barrett et al., 2007). As previously discussed, any wind-blown material close to the surface which is derived from the relatively young, P-rich soils of Explorer's Cove likely remains coastal due to potential blockage of surface winds by Coral Ridge. This does not mean that the inner valley floor does not experience the influence from easterly winds, as it has been clearly documented that they do (Doran et al., 2002), but it does strongly suggest that the easterlies do not sufficiently entrain coastal soils and transport them inland. Also, because of the limited fetch over land of the easterlies, the source area for the entrainment of material is also limited. The bottommost samples from F6 and Miers Valley, which have nutrient ratios intermediate between the coastal and further inland sites, and are near young soils with high P concentrations, are relatively more P enriched than top and middle samples and thus are likely potential inland P sources.

The aeolian material at East Lake Bonney was differentiated based on season by its N:P ratio (Figure 8), where winter samples were above the Redfield stoichiometric ratio of N:P = 16:1 line, implying potential N enrichment, while full-year samples were below the Redfield line, implying potential P enrichment for aquatic ecosystems. This indicates that at certain times of high onshore winds, some finer-grained material from the P-enriched soils in the Fryxell Basin is transported into the Bonney Basin or that there is another higher-elevation source of P-enriched material being transported. Little information is available on P concentrations in the higher-elevation Transantarctic Mountains soils, but what do exist would negate the latter idea. Therefore, the source of these higher P:N ratio materials is an enigma at this time.

Though down-valley transported NO_3^- could be important for young soil ecosystems, Deuerling et al. (2014) reported aeolian fluxes of water-soluble nutrients from 30 cm above the surface at 6 times less than the flux of nutrients to aquatic systems from MDV soils (Barrett et al., 2007). Water-soluble N and P data from this study and sediment flux data from Lancaster (2002) and Šabacká et al. (2012) were used to estimate N and P fluxes at 30 and 100 cm above the ground surface (Table 3). The 100-cm N fluxes were about 10 times lower than values from Deuerling et al. (2014) at 30 cm, while P fluxes were similar. Overall, soluble N and P aeolian fluxes are between 100 and 1,000 times lower than the fluxes of nutrients from soils to aquatic ecosystems, as calculated by Barrett et al. (2007). Due to their lower concentrations compared to Taylor Valley soils, the input of aeolian materials to streams and lake edges probably has little ecological consequence. However, as earlier

Table 3
Total Sediment Flux From Previous Studies in the McMurdo Dry Valleys

Location	Total sediment flux ($\text{g}\cdot\text{m}^{-2}\cdot\text{year}^{-1}$)	Height of collection (cm)	Years of collection	Soluble N flux ($\mu\text{mol}\cdot\text{m}^{-2}\cdot\text{year}^{-1}$)	Soluble P flux ($\mu\text{mol}\cdot\text{m}^{-2}\cdot\text{year}^{-1}$)
Lancaster, 2002					
Explorer's Cove	27.87	100	1997–2000	0.94 ^a	0.34 ^a
Lake Fryxell	1.00	100	1997–2000	0.21 ^a	0.00 ^a
Lake Hoare	0.86	100	1997–2000	—	—
Lake Bonney	110.53	100	1997–2000	4.04 ^a	0.20 ^a
Lake Brownworth	441.80	100	1997–2000	—	—
Lake Vanda	227.50	100	1997–2000	—	—
Lake Vida	39.56	100	1997–2000	—	—
Commonwealth Glacier	0.26	100	1997–2000	—	—
Canada Glacier	0.43	100	1997–2000	—	—
Howard Glacier	0.47	100	1997–2000	—	—
Taylor Glacier	3.73	100	1997–2000	1.53 ^a	0.00 ^a
Šabacká et al., 2012					
Lake Fryxell	72.3	30	1998–2008	7.74 ^b	0.23 ^b
Lake Hoare	289	30	1999–2008	—	—
West Lake Bonney	8.50	30	1999–2008	0.48 ^b	0.01 ^b
Atkins & Dunbar, 2009					
McMurdo Sound	7.76–24.5	0	2006–2007	—	—

^aN and P fluxes were calculated using 100-cm sediment flux data from Lancaster (2002) and ~100-cm collection height chemistry from this study. ^bN and P fluxes were calculated using 20-cm sediment flux data from Šabacká et al. (2012) and ~30-cm collection height chemistry data from this study.

work on glacier and lake ice surfaces (Fountain et al., 2004; Priscu, 1995; Priscu et al., 1999), as well as cryoconites (Bagshaw et al., 2007; Porazinska et al., 2004) have concluded, if aeolian material deposited onto these surfaces later comes into contact with liquid water, this material has the potential to provide important, new sources of N and P to cryoconite, stream, and lake ecosystems.

5. Conclusions

The geochemistry of soluble salts and nutrients in aeolian material from the MDV generally reflects the complicated geologic and climate history of the Ross Sea region, as well as the surficial soil ages of the valleys where some of the soluble fraction is derived. This material does vary spatially with respect to height above the surface, distance from the ocean, and elevation but does not vary significantly seasonally. Lower collection height samples (~5–20 cm) demonstrate little intervalley connectivity, while the uppermost samples (~100 cm) demonstrate some mixing, altering the chemical continuum.

Material in Taylor Valley is generally transported down valley from Taylor Glacier toward the coast. Though there are summer up-valley winds, they mainly affect coastal areas and do not appear to transport enough material up valley to significantly alter the composition of aeolian material at inland locations, except potentially regarding nutrient transport. Nitrate rich material originating from the higher-elevation, inland locations may help to support younger N-limited soils, while lower elevations in Taylor Valley could be source of phosphorus for older P-limited soils as far inland as East Lake Bonney during times of high particle transport. Salt concentrations varied with collection height, where NO_3^- and Cl^- concentrations were the highest at the uppermost collection height, even for the distant and high-elevation locations. This suggests that materials at these heights are likely entrained longer than materials closer to the surface and hence have accumulated marine aerosols and atmospherically derived nitrate on grain surfaces.

References

- Adams, E. E., Priscu, J. C., Fritsen, C. H., Smith, S. R., & Brackman, S. L. (1998). Permanent ice covers of the McMurdo Dry Valleys lakes, Antarctica: Bubble formation and metamorphism. In J. C. Priscu (Ed.), *Ecosystem dynamics in a polar desert: The McMurdo Dry Valleys, Antarctica, Antarctic Research Series*, (Vol. 72, pp. 281–295). Washington, D. C: American Geophysical Union.
- Atkins, C. B., & Dunbar, G. B. (2009). Aeolian sediment flux from sea ice into southern McMurdo Sound, Antarctica. *Global and Planetary Change*, 69(3), 133–141. <https://doi.org/10.1016/j.gloplacha.2009.04.006>
- Bagshaw, E. A., Tranter, M., Fountain, A. G., Welch, K. A., Basagic, H., & Lyons, W. B. (2007). Biogeochemical evolution of cryoconite holes on Canada Glacier, Taylor Valley, Antarctica. *Journal of Geophysical Research*, 112, G04S35. <https://doi.org/10.1029/2007JG000442>

Acknowledgments

This work was supported by the National Science Foundation grant ANT 1115245 awarded to W. Berry Lyons for the McMurdo Dry Valleys Long Term Ecological Research (MCM-LTER). Supporting data are included as four tables and eight figures in the supporting information; any additional data may be obtained from the McMurdo LTER website (mcm.lter.org). We express our gratitude to an anonymous reviewer and Gavin Dunbar for their thoughtful comments, which have greatly improved the manuscript, and additionally thank ASC for logistical support and PHI for helicopter support.

- Barrett, J. E., Virginia, R. A., Lyons, W. B., McKnight, D. M., Priscu, J. C., Doran, P. T., Fountain, A. G., et al. (2007). Biogeochemical stoichiometry of Antarctic Dry Valley ecosystems. *Journal of Geophysical Research*, 112, G01010. <https://doi.org/10.1029/2005JG000141>
- Barrett, J. E., Virginia, R. A., Parsons, A. N., & Wall, D. H. (2005). Potential soil organic matter turnover in Taylor Valley, Antarctica. *Arctic, Antarctic, and Alpine Research*, 37(1), 108–117. [https://doi.org/10.1657/1523-0430\(2005\)037\[0108:PSOMTI\]2.0.CO;2](https://doi.org/10.1657/1523-0430(2005)037[0108:PSOMTI]2.0.CO;2)
- Bisson, K. M., Welch, K. A., Welch, S. A., Sheets, J. M., Lyons, W. B., Levy, J. S., & Fountain, A. G. (2015). Patterns and processes of salt efflorescences in the McMurdo region, Antarctica. *Arctic, Antarctic, and Alpine Research*, 47(3), 407–425. <https://doi.org/10.1657/AAAR0014-024>
- Bockheim, J. G., & McLeod, M. (2007). Soil distribution in the McMurdo Dry Valleys, Antarctica. *Geoderma*, 18(3), 217–227. <https://doi.org/10.1002/ppp.588>
- Calkin, P. E. (1964). Geomorphology and glacial geology of the Victoria Valley system, southern Victoria Land, Antarctica. *Institute of Polar Studies Report 10, Research Foundation and Institute of Polar Studies, The Ohio State University*, 102 pages.
- Chadwick, O. A., Derry, L. A., Vitousek, P. M., Huebert, B. J., & Hedin, L. O. (1999). Changing sources of nutrients during four million years of ecosystem development. *Nature*, 397(6719), 491–497. <https://doi.org/10.1038/17276>
- Clow, G. D., McKay, C. P., Simmons, G. M. Jr., & Wharton, R. A. Jr. (1988). Climatological observations and predicted sublimation rates at Lake Hoare, Antarctica. *Journal of Climatology*, 1(7), 715–728. [https://doi.org/10.1175/1520-0442\(1988\)001<0715:COAPSR>2.0.CO;2](https://doi.org/10.1175/1520-0442(1988)001<0715:COAPSR>2.0.CO;2)
- Craddock, C. (1970). *Geologic maps of Antarctica, Antarctic Map Folio Series*, (Vol. 12, p. 6). New York: American Geographical Society.
- Denton, G. H., Bockheim, J. G., Wilson, S. C., & Stuiver, M. (1989). Late Wisconsin and Early Holocene glacial history, inner Ross embayment, Antarctica. *Quaternary Research*, 31(02), 151–182. [https://doi.org/10.1016/0033-5894\(89\)90004-5](https://doi.org/10.1016/0033-5894(89)90004-5)
- Deuerling, K. M. (2010). Aeolian sediments of the McMurdo Dry Valleys, Antarctica. *School of Earth Sciences, The Ohio State University, MS Thesis*, 164 pages.
- Deuerling, K. M., Lyons, W. B., Welch, S. A., & Welch, K. A. (2014). The characterization and role of aeolian deposition on water quality, McMurdo Dry Valleys, Antarctica. *Aeolian Research*, 13, 7–17. <https://doi.org/10.1016/j.aeolia.2014.01.002>
- Dickson, J. L., Head, J. W., Levy, J. S., & Marchant, D. R. (2013). Don Juan Pond, Antarctica: Near-surface CaCl₂-brine feeding Earth's most saline lake and implications for Mars. *Scientific Reports*, 3(1), 1166. <https://doi.org/10.1038/srep01166>
- Doran, P. T., McKay, C. P., Clow, G. D., Dana, G. L., Fountain, A. G., Nysten, T., & Lyons, W. B. (2002). Valley floor climate observations from the McMurdo Dry Valleys, Antarctica, 1986–2000. *Journal of Geophysical Research*, 107(D24), 4772. <https://doi.org/10.1029/2001JD002045>
- Doran, P. T., Wharton, R. A. Jr., & Lyons, W. B. (1994). Paleolimnology of the McMurdo Dry Valleys, Antarctica. *Journal of Paleolimnology*, 10(2), 85–114. <https://doi.org/10.1007/BF00682507>
- Foley, K. K., Lyons, W. B., Barrett, J. E., & Virginia, R. A. (2006). Pedogenic carbonate distribution within glacial till in Taylor Valley, southern Victoria Land, Antarctica. In A. M. Alonso-Zarza & L. H. Tanner (Eds.), *Paleoenvironmental record and applications of calcretes and palustrine carbonates, Geological Society of America Special Paper*, (Vol. 416, pp. 89–103). [https://doi.org/10.1130/2006.2416\(06\)](https://doi.org/10.1130/2006.2416(06))
- Fortner, S. K., Tranter, M., Fountain, A. G., Lyons, W. B., & Welch, K. A. (2005). The geochemistry of supraglacial streams of Canada Glacier, Taylor Valley (Antarctica), and their evolution into proglacial waters. *Aquatic Geochemistry*, 11(4), 391–412. <https://doi.org/10.1007/s10498-004-7373-2>
- Fountain, A. G., Levy, J. S., Gooseff, M. N., & Van Horn, D. (2014). The McMurdo Dry Valleys: A landscape on the threshold of change. *Geomorphology*, 225, 25–35. <https://doi.org/10.1016/j.geomorph.2014.03.044>
- Fountain, A. G., Lyons, W. B., Burkins, M. B., Dana, G. L., Doran, P. T., Lewis, K. J., McKnight, D. M., et al. (1999). Physical controls on the Taylor Valley ecosystem, Antarctica. *Bioscience*, 49(12), 961–971. <https://doi.org/10.1525/bisi.1999.49.12.961>
- Fountain, A. G., Nysten, T. H., Monaghan, A., Basagic, H. J., & Bromwich, D. (2010). Snow in the McMurdo Dry Valleys, Antarctica. *International Journal of Climatology*, 30, 633–642. <https://doi.org/10.1002/joc.1933>
- Fountain, A. G., Tranter, M., Nysten, T. H., Lewis, K. J., & Mueller, D. R. (2004). Evolution of cryoconite holes and their contribution to meltwater runoff from glaciers in the McMurdo Dry Valleys, Antarctica. *Journal of Glaciology*, 50(168), 35–45. <https://doi.org/10.3189/172756504781830312>
- Fristen, C. H., Grue, A. M., & Priscu, J. C. (2000). Distribution of organic carbon and nitrogen in surface soils in the McMurdo Dry Valleys, Antarctica. *Polar Biology*, 23(2), 121–128. <https://doi.org/10.1007/s003000050017>
- Gillies, J. A., Nickling, W. G., & Tilson, M. (2013). Frequency, magnitude, and characteristics of aeolian sediment transport: McMurdo Dry Valleys, Antarctica. *Journal of Geophysical Research: Earth Surface*, 118, 461–479. <https://doi.org/10.1002/jgrf.20007>
- Gooseff, M. N., Blum, A. E., Lyons, W. B., & McKnight, D. M. (2002). Weathering reactions and hyporheic exchange controls on stream water chemistry in a glacial meltwater stream in the McMurdo Dry Valleys. *Water Resources Research*, 38(12), 1279. <https://doi.org/10.1029/2001WR000834>
- Hall, B. L., Denton, G. H., & Hendy, C. H. (2000). Evidence from Taylor Valley for a grounded ice sheet in the Ross Sea, Antarctica. *Geografiska Annaler*, 82(2-3), 275. <https://doi.org/10.1111/j.0435-3676.2000.00126.x-303>
- Hall, B. L., Denton, G. H., Lux, D. R., & Bockheim, J. G. (1993). Late Tertiary Antarctic paleoclimate and ice-sheet dynamics inferred from surficial deposits in Wright Valley. *Geografiska Annaler*, 75(4), 239–268. <https://doi.org/10.2307/521203>
- Hall, B. L., Denton, G. H., Stone, J. O., & Conway, H. (2013). History of the grounded ice sheet in the Ross Sea sector of Antarctica during the Last Glacial Maximum and the last termination. *Geological Society, London, Special Publications*, 381(1), 167–181. <https://doi.org/10.1144/SP381.5>
- Honda, M., Yabuki, S., & Shimizu, H. (2004). Geochemical and isotopic studies of aeolian sediments in China. *Sedimentology*, 51(2), 211–230. <https://doi.org/10.1111/j.1365-3091.2004.00618.x>
- Jickells, T. D., An, Z. S., Andersen, K. K., Baker, A. R., Bergametti, G., Brooks, N., Cao, J. J., et al. (2005). Global iron connections between desert dust, ocean biogeochemistry, and climate. *Science*, 308(5718), 67–71. <https://doi.org/10.1126/science.1105959>
- Kelley, W. P. (1951). *Alkali soils: Their formation, properties and reclamation*, (Vol. 72, p. 403). New York: Reinhold Publishing Corporation. <https://doi.org/10.1097/00010694-195111000-00008>
- Keys, J. R., & Williams, K. (1981). Origin of crystalline, cold desert salts in the McMurdo region, Antarctica. *Geochimica et Cosmochimica Acta*, 45(12), 2299–2309. [https://doi.org/10.1016/0016-7037\(81\)90084-3](https://doi.org/10.1016/0016-7037(81)90084-3)
- Khan, A. L., Jaffe, R., Ding, Y., & McKnight, D. M. (2016). Dissolved black carbon in Antarctic lakes: Chemical signatures of past and present sources. *Geophysical Research Letters*, 43, 5750–5757. <https://doi.org/10.1002/2016GL068609>
- Kyle, P. R. (1990). McMurdo volcanic group, western Ross embayment. In W. E. Le Masurier & J. W. Thomson (Eds.), *Volcanoes of the Antarctic Plate of the Southern Oceans, Antarctic Research*, (Vol. 48, pp. 1–17). Washington, D. C.: American Geophysical Union. <https://doi.org/10.1029/AR048p0018>
- Lancaster, N. (2002). Flux of eolian sediment in the McMurdo Dry Valleys, Antarctica: A preliminary assessment. *Arctic and Antarctic Alpine Research*, 34(3), 318–323. <https://doi.org/10.2307/1552490>

- Lancaster, N., Nickling, W. G., & Gillies, J. A. (2010). Sand transport by wind on complex surfaces: Field studies in the McMurdo Dry Valleys, Antarctica. *Journal of Geophysical Research*, *115*, F03027. <https://doi.org/10.1029/2009JF001408>
- Levy, J. S., Fountain, A. G., Welch, K. A., & Lyons, W. B. (2012). Hypersaline "wet patches" in Taylor Valley, Antarctica. *Geophysical Research Letters*, *39*, L05402. <https://doi.org/10.1029/2012GL050898>
- Lyons, W. B., Welch, K. A., Neumann, K., Toxey, J. K., McArthur, R., Williams, C., et al. (1998). Geochemical linkages among glaciers, streams, and lakes within the Taylor Valley, Antarctica. In J. C. Priscu (Ed.), *Ecosystem Dynamics in a Polar Desert: The McMurdo Dry Valleys, Antarctica* (pp. 77–92). Washington, DC: American Geophysical Union. <https://doi.org/10.1029/AR072p0077>
- Lyons, W. B., Deuerling, K. M., Welch, K. A., Welch, S. A., Michalski, G., Walters, W. W., Nielsen, U., et al. (2016). The soil geochemistry in the Beardmore Glacier region, Antarctica: Implications for terrestrial ecosystem history. *Scientific Reports*, *6*(1), 26189. <https://doi.org/10.1038/srep26189>
- Lyons, W. B., Fountain, A. G., Doran, P., Priscu, J. C., Neumann, K., & Welch, K. A. (2000). Importance of landscape position and legacy: The evolution of the lakes in Taylor Valley, Antarctica. *Freshwater Biology*, *43*(3), 355–367. <https://doi.org/10.1046/j.1365-2427.2000.00513.x>
- Lyons, W. B., & Mayewski, P. A. (1993). The geochemical evolution of terrestrial waters in the Antarctic: The role of rock-water interactions. In W. J. Green & E. I. Friedmann (Eds.), *Physical and biogeochemical processes in Antarctic lakes* (pp. 135–143). Washington, D. C: American Geophysical Union. <https://doi.org/10.1029/AR059p0135>
- Lyons, W. B., Welch, K. A., Fountain, A. G., Dana, G., & Vaughn, B. H. (2003). Surface glaciochemistry of Taylor Valley, southern Victoria Land, Antarctica and its effect on stream chemistry. *Hydrological Processes*, *17*(1), 115–130. <https://doi.org/10.1002/hyp.1205>
- Lyons, W. B., Welch, K. A., Gardner, C. B., Jaros, C., Moorhead, D. L., Knoepfle, J. L., & Doran, P. T. (2012). The geochemistry of upland ponds, Taylor Valley, Antarctica. *Antarctic Science*, *24*(01), 3–14. <https://doi.org/10.1017/S0954102011000617>
- Marchant, D. R., & Denton, G. H. (1996). Miocene and Pliocene paleoclimate of the Dry Valleys region, southern Victoria Land: A geomorphological approach. *Marine Micropaleontology*, *27*(1–4), 253–271. [https://doi.org/10.1016/0377-8398\(95\)00065-8](https://doi.org/10.1016/0377-8398(95)00065-8)
- McKnight, D. M., Niyogi, D. K., Alger, A. S., Bombliies, A., Conovitz, P. A., & Tate, C. M. (1999). Dry Valley streams in Antarctica: Ecosystems waiting for water. *Bioscience*, *49*(12), 985–995. <https://doi.org/10.2307/1313732>
- Moorhead, D. L., Doran, P. T., Fountain, A. G., Lyons, W. B., McKnight, D. M., Priscu, J. C., Virginia, R. A., et al. (1999). Ecological legacies: Impacts on ecosystems of the McMurdo Dry Valleys. *Bioscience*, *49*(12), 1009–1019. <https://doi.org/10.1525/bisi.1999.49.12.1009>
- Nkem, J. N., Virginia, R. A., Barrett, J. E., Wall, D. H., & Li, G. (2006). Salt tolerance and survival thresholds for two species of Antarctic soil nematodes. *Polar Biology*, *29*(8), 643–651. <https://doi.org/10.1007/s00300-005-0101-6>
- Nylen, T. H., Fountain, A. G., & Doran, P. T. (2004). Climatology of katabatic winds in the McMurdo Dry Valleys, southern Victoria Land, Antarctica. *Journal of Geophysical Research*, *109*, D03114. <https://doi.org/10.1029/2003JD003937>
- Obyrk, M. K., Doran, P. T., Waddington, E. D., & McKay, C. P. (2017). The influence of föhn winds on glacial Lake Washburn and palaeotemperatures in the McMurdo Dry Valleys, Antarctica, during the Last Glacial Maximum. *Antarctic Science*, *29*(05), 457–467. <https://doi.org/10.1017/S0954102017000062>
- Okin, G. S., Gillette, D. A., & Herrick, J. E. (2006). Multi-scale controls on and consequences of aeolian processes in landscape change in arid and semi-arid environments. *Journal of Arid Environments*, *65*(2), 253–275. <https://doi.org/10.1016/j.jaridenv.2005.06.029>
- Porazinska, D. L., Fountain, A. G., Nylen, T. H., Tranter, M., Virginia, R. A., & Wall, D. H. (2004). The biodiversity and biogeochemistry of cryoconite holes from McMurdo Dry Valley Glaciers, Antarctica. *Arctic, Antarctic, and Alpine Research*, *36*(1), 84–91. [https://doi.org/10.1657/1523-0430\(2004\)036\[0084:TBABOC\]2.0.CO;2](https://doi.org/10.1657/1523-0430(2004)036[0084:TBABOC]2.0.CO;2)
- Prentice, M. L., Kleman, J., & Stroeven, J. P. (1998). The composite glacial erosional landscape of the northern McMurdo Dry Valleys: Implications for Antarctic Tertiary glacial history. In J. C. Priscu (Ed.), *Ecosystem dynamics in a polar desert: The McMurdo Dry Valleys, Antarctica, Antarctic Research Series*, (Vol. 72, pp. 1–38). Washington, D. C: American Geophysical Union. <https://doi.org/10.1029/AR072p0001>
- Priscu, J. C. (1995). Phytoplankton nutrient deficiency in lakes of the McMurdo Dry Valleys, Antarctica. *Freshwater Biology*, *34*(2), 215–227. <https://doi.org/10.1111/j.1365-2427.1995.tb00882.x>
- Priscu, J. C., Wolf, D. F., Takacs, C. D., Fritsen, C. H., Laybourn-Parry, J., Roberts, E. C., Sattler, B., et al. (1999). Carbon transformations in a perennially ice-covered Antarctic lake. *Bioscience*, *49*(12), 997–1008. <https://doi.org/10.1525/bisi.1999.49.12.997>
- R Core Team (2013). *R: A language and environment for statistical computing*. Vienna, Austria: R Foundation for Statistical Computing. URL <http://www.R-project.org/>
- Šabacká, M., Priscu, J. C., Basagic, H. J., Fountain, A. G., Wall, D. H., Virginia, R. A., & Greenwood, M. C. (2012). Aeolian flux of biotic and abiotic material in Taylor Valley, Antarctica. *Geomorphology*, *155–156*, 102–111. <https://doi.org/10.1016/j.geomorph.2011.12.009>
- Shao, Y., Mctainsh, G. H., Leys, J. F., & Raupach, M. R. (1993). Efficiencies of sediment samplers for wind erosion measurement. *Soil Research*, *31*(4), 519–532. <https://doi.org/10.1071/SR9930519>
- Toner, J. D., Sletten, R. S., & Prentice, M. L. (2013). Soluble salt accumulations in Taylor Valley, Antarctica: Implications for paleolakes and Ross Sea ice sheet dynamics. *Journal of Geophysical Research: Earth Surface*, *118*, 198–215. <https://doi.org/10.1029/2012JF002467>
- Vitousek, P., Chadwick, O., Crew, T., Fownes, J., Hendrick, D., & Herbert, D. (1997). Soil and ecosystem development across the Hawaiian Islands. *GSA Today*, *7*, 1–9.
- Wei, T., Dong, Z., Kang, S., Qin, X., & Guo, Z. (2017). Geochemical evidence for sources of surface dust deposited on the Laohugou Glacier, Qilian Mountains. *Applied Geochemistry*, *79*, 1–8. <https://doi.org/10.1016/j.apgeochem.2017.01.024>
- Welch, K. A., Lyons, W. B., Graham, E., Neumann, K., Thomas, J. M., & Mikesell, D. (1996). Determination of major element chemistry in terrestrial waters from Antarctica by ion chromatography. *Journal of Chromatography*, *739*, 257–263. [https://doi.org/10.1016/0021-9673\(96\)00044-1](https://doi.org/10.1016/0021-9673(96)00044-1)
- Welch, K. A., Lyons, W. B., Whisner, C., Gardner, C. B., Gooseff, M. N., McKnight, D. M., & Priscu, J. C. (2010). Spatial variations in the geochemistry of glacial meltwater streams in the Taylor Valley, Antarctica. *Antarctic Science*, *22*(06), 662–672. <https://doi.org/10.1017/S0954102010000702>
- Wilch, T. I., Lux, D. R., Denton, G. H., & McIntosh, W. C. (1993). Minimal Pliocene-Pleistocene uplift of the Dry Valleys sector of the Transantarctic Mountains: A key parameter in ice sheet reconstructions. *Geology*, *21*(9), 841–844. [https://doi.org/10.1130/0091-7613\(1993\)021<0841:MPPUOT>2.3.CO;2](https://doi.org/10.1130/0091-7613(1993)021<0841:MPPUOT>2.3.CO;2)
- Wilson, A. T. (1979). Geochemical problems of the Antarctic dry areas. *Nature*, *280*(5719), 205–208. <https://doi.org/10.1038/280205a0>
- Witherow, R. A., Lyons, W. B., Bertler, N. A. N., Welch, K. A., Mayewski, P. A., Sneed, S. B., Nylen, T., et al. (2006). The aeolian flux of calcium, chloride and nitrate to the McMurdo Dry Valleys landscape: Evidence from snow pit analysis. *Antarctic Science*, *18*(04), 497–505. <https://doi.org/10.1017/S095410200600054X>
- Xu, J., Yu, G., & Kang, S. (2012). Sr-Nd isotope evidence for modern aeolian dust sources in mountain glaciers of western China. *Journal of Glaciology*, *58*(211), 859–865. <https://doi.org/10.3189/2012JG12J006>